Effect of uniaxial stress on photoluminescence in GaN and stimulated emission in $In_xGa_{1-x}N$/GaN multiple quantum wells

Masayoshi Ichimiya, Masayuki Watanabe, Tokiko Ohata, and Tetsusuke Hayashi
Faculty of Integrated Human Studies, Kyoto University, Kyoto 606-8501, Japan

Akihiko Ishibashi
Advanced Technology Research Laboratories, Matsushita Electric Industrial Co., Ltd., Moriguchi, Osaka 570-8501, Japan

(Received 26 November 2002; revised manuscript received 6 May 2003; published 29 July 2003)

Photoluminescence and stimulated emission (SE) in a wurtzite GaN bulk crystal and $In_xGa_{1-x}N$/GaN multiple quantum wells (MQW's) are investigated under uniaxial stress applied perpendicularly to the *c* axis. The strain in GaN induces a decrease in the photoluminescence intensity of *B* excitons relative to *A* excitons due to an increase in the energy splitting between the two states. In $In_xGa_{1-x}N$/GaN MQW's, SE and optical gain in the localized states are observed at 6 K under low excitation power below the Mott density of excitons. The uniaxial stress induces a low-energy shift of the gain peak and a decrease in the threshold carrier density of SE. In the excitation power above the Mott density, the SE arises from an electron-hole plasma recombination. The gain value at 0.43 GPa is 1.34 times as large as that without stress at 6 K, which is comparable with a theoretical estimation. The observed effects of strain are ascribed to a decrease in the density of states at the valance-band maximum.

DOI: 10.1103/PhysRevB.68.035328 PACS number(s): 78.45.+h, 78.55.Cr, 71.70.Fk, 81.05.Ea

I. INTRODUCTION

III-V compounds have been widely utilized for materials of semiconductor light emitting diodes (LED's) or laser diodes (LD's). The mixed crystals based on GaAs have been used for lasers in the region from infrared to visible light.[1–3] In recent years, III-V nitride compounds based on GaN have attracted attention for materials emitting blue to ultraviolet light.[4–9] However, it has been pointed out that high carrier density is required to generate the optical gain compared with the GaAs family.[10,11] This is due to the large effective masses in both conduction and valence bands of GaN; the strong electron affinity and the weak spin-orbit coupling of nitrogen atoms yield large electron and hole effective masses. The high density of states due to the heavy masses requires high carrier density to achieve the population inversion.[12]

Suzuki and Uenoyama investigated electronic band structures with the derivation of effective-mass parameters from first-principles calculations for zinc-blende GaN as well as for wurtzite GaN and AlN.[13–15] They investigated the strain effect on wurtzite and zinc-blende GaN/AlGaN quantum wells whose valence-subband structures were studied using the $\mathbf{k}\cdot\mathbf{p}$ method.[16–20] It was shown that a biaxial strain is not so effective for the reduction of threshold carrier density to generate stimulated emission (SE) in wurtzite wells, while it reduces the threshold density in zinc-blende wells. On the contrary, a uniaxial strain into the *c* plane of wurtzite wells is useful for reducing the threshold carrier density of SE.

In wurtzite GaN, the valence band near the Γ point splits into two states by the crystal field. One of them is of Γ_1 symmetry and the other of Γ_6 symmetry, and the latter further splits into two states due to spin-orbit interaction.[13–16] The former state is called the *C* band (Γ_7) and the latter two states are called the *A* band (Γ_7) and *B* band (Γ_9). The energy of the *A* band is slightly higher than that of the *B* band, and that of the *C* band is low compared with the *A* and *B* bands. Three kinds of excitons called *A*, *B*, and *C* excitons are formed corresponding to each valence band. A uniaxial stress introduced perpendicularly to the *c* axis gives rise to the structural change of crystal from C_6 to C_2. This change increases the energy splitting between the *A* and *B* bands and induces a decrease in the density of states at the Γ point.[18–20] Yamaguchi it et al. measured the dependence of the reflectance spectrum on the uniaxial stress in bulk wurtzite GaN and showed that the energy splitting between *A* and *B* excitons increases with uniaxial stress applied in the *c* plane.[21]

Suzuki and Uenoyama also calculated the influence of uniaxial strain on the optical gain in wurtzite GaN.[18–20] They concluded that the optical gain increases with strain due to the decrease in the density of states and that the effect is remarkable in GaN/AlGaN quantum wells. Domen *et al.* also reported a similar result.[22] However, experimental studies of the strain effect on the photoluminescence (PL) and optical gain have not been reported so far.

Quantum wells using mixed crystals of InGaN for the active layers have been attracting much attention for practical fabrication of bluish light-emitting devices. This is owing to the tunability of the wavelength with In content and the high quantum efficiency by virtue of carrier localization. The PL at low temperatures with low excitation density is characterized by the localization effect peculiar to mixed crystals as well as by the Stark effect due to quantum well structures.[23–28] Efforts have been devoted to clarify the mechanism of SE. It has been demonstrated that the SE at low temperatures arises from the localized exciton (LE) PL.[24,29] It was also reported that a recombination of *e-h* plasma contributes to SE at room temperature.[30,31] It is supposed that, in spite of the localization effect in the mixed crystal, the nature of the electronic structure of GaN is essentially maintained as far as the In content is not so high. In

fact, a strong transverse electric polarization was observed in the SE arising from the polarization selection rule of the *A* exciton in InGaN multiple quantum wells (MQW's).[30] Therefore, it is expected that the effect of strain on the band structure would appear on the PL and optical gain in InGaN systems.

In this paper, we investigate the stress dependence of the exciton luminescence in a GaN crystal and of the SE and optical gain in InGaN/GaN MQW's. The effect of stress is compared for the cases of low and high carrier densities. The stress effect on the SE at room temperature is also observed in InGaN/GaN MQW's.

II. EXPERIMENTAL PROCEDURE

The samples were grown by low-pressure (300 Torr) metalorganic vapor phase epitaxy (MOVPE) on a (0001)-oriented sapphire substrate. Here 1.0-μm-thick undoped-GaN epilayers were grown using a 40-nm-thick low-temperature GaN buffer layer. InGaN/GaN MQW's were grown on the GaN epilayer with a 15-nm-thick GaN capping layer. The MQW's are constructed of five periods of 2.5-nm-thick undoped-InGaN active layers with 7.5-nm-thick GaN barrier layers. The indium content of InGaN wells is 10%.

PL in a GaN bulk crystal was measured with a He-Cd laser for the excitation, which was incident almost normal to the *c* surface of the sample and focused in the shape of spot. SE was measured with a N_2 laser, which was incident normal to the *c* surface and focused in the shape of a transverse stripe using a cylindrical lens to amplify the SE. As the detector, a monochromator equipped with an optical multichannel analyzer was set in the direction perpendicular to the *c* axis to catch the amplified SE. Optical gain was obtained from the SE spectra measured with varying the stripe length with a mask in front of the sample. The cavity effect was negligible in this configuration.

Compressive uniaxial stress was introduced to the sample by a spring-loaded stress system mounted in a He-flow-type cryostat. It was directed perpendicular to the *c* axis and was also perpendicular to the direction of light output propagating into the detector. The value of stress was monitored with a strain-gauge transducer inserted in the system.

III. RESULTS AND DISCUSSION

A. Stress effect on exciton luminescence in GaN

Figure 1 shows the uniaxial stress dependence of the PL spectrum in a GaN bulk crystal. The temperature was set to 50 K to make the *A*- and *B*-exciton PL bands clear by reducing the bound exciton luminescence which is dominant below 50 K. The values of uniaxial stress are displayed at the right side of the spectra. Dotted lines correspond to the peak energies of *A*-exciton PL (E_A) and *B*-exciton PL (E_B) which were determined from the decomposition of spectra with two Lorentzian functions. Though the Lorentzian function might not be exact enough for the exciton PL spectra, the obtained *A*- and *B*-exciton energies are coincident with those obtained from the reflection spectra measured under the same stress and also with those reported by Yamaguchi *et al.*[21] E_A is almost unchanged, while E_B shifts to higher energy as the stress is increased. It is clear that distortion of the *c* plane leads to an increase in the splitting between E_A and E_B (E_{AB}).

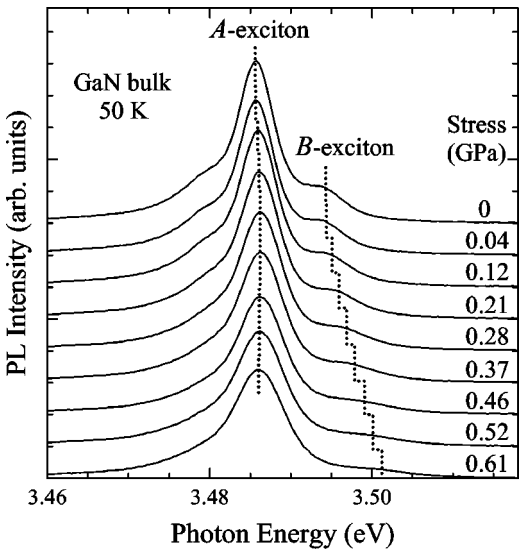

FIG. 1. Uniaxial stress dependence of the PL spectrum at 50 K in GaN. The dotted lines correspond to the peak energies of *A*-exciton (E_A) and *B*-exciton (E_B) PL bands.

The solid squares in Fig. 2 show the PL intensity of *B* excitons relative to that of *A* excitons, I_B/I_A, derived from the integrated intensities of two Lorentzians fitted to the spectrum in Fig. 1. The abscissa shows the uniaxial stress applied to the sample. The relative intensity decreases monotonically against the stress. If thermal equilibrium is established and the probability distribution of excitons follows the Boltzmann distribution, the ratio of *B*-exciton density (n_B) to *A*-exciton density (n_A) decreases as

$$n_B = n_A \exp(-E_{AB}/k_B T), \tag{1}$$

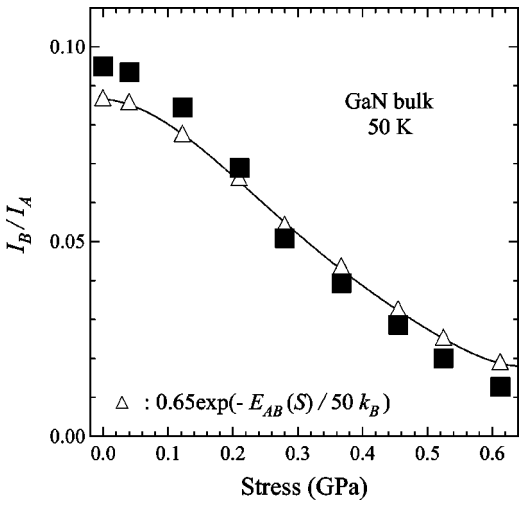

FIG. 2. Intensity of *B*-exciton PL relative to that of *A*-exciton PL of GaN (I_B/I_A) at 50 K plotted against the stress (solid squares). Open triangles are the calculated one with E_{AB} (S) in Fig. 1.

where k_B and T are Boltzmann constant and temperature, respectively. E_{AB} can be expressed as a function of stress (S), and the stress dependence of I_B/I_A is given by

$$I_B/I_A = a \exp(-E_{AB}(S)/k_B T), \quad (2)$$

where a is a fitting parameter. The experimental result can be approximated by Eq. (2) using E_{AB} (S) derived from Fig. 1, as shown by open triangles in Fig. 2. The observed change in the PL spectrum with the application of stress can be ascribed to a population change in A and B excitons.

B. Stress effect on stimulated emission in InGaN/GaN MQW's

The excitation power dependence of PL spectrum in $In_{0.1}Ga_{0.9}N$/GaN MQW's was measured at 6 K with tuning the power between 4.25 kW/cm^2 and 704 kW/cm^2. The estimated sheet carrier density (SCD) is between 4.8×10^{10} cm^{-2} and 8.0×10^{12} cm^{-2} with the assumption that the exciton lifetime is 100 ps and the absorption coefficient at the excitation photon energy is the same as that in GaN (1.0×10^5 cm^{-1}).[32] Several spectra (from 26.2 kW/cm^2 to 109 kW/cm^2) are displayed in Fig. 3 to emphasize the transition of the spectral feature. The results under uniaxial stress of 0 GPa, 0.22 GPa, and 0.43 GPa are shown in (a), (b), and (c), respectively. The peak intensity of each spectrum for the lowest excitation power (26.2 kW/cm^2) is set to unity. The shapes of the spectra for 26.2 kW/cm^2 in (a), (b), and (c) are almost the same in the region below the peak energy. However, the width of the higher-energy side of the spectrum decreases with increasing stress. The transverse arrows indicate the width at half maximum, and the values are 23.2 meV, 22.0 meV, and 20.8 meV in (a), (b), and (c), respectively. The PL with a single broadband is LE-PL, which contains components corresponding to A- and B-exciton PL in GaN. The reduction of the width in the high-energy side is attributed to a decrease in the component of B excitons relative to that of A excitons similar to the case for GaN in the previous section.

In Fig. 3(a), the spectrum has the shape of a broadband under excitation power from 26.2 kW/cm^2 to 46.8 kW/cm^2. Above 61.8 kW/cm^2 (SCD of 7.0×10^{11} cm^{-2}), a sharp nonlinear component corresponding to SE appears at the high-energy side of the band. The results with a uniaxial stress [(b) and (c)] are the same as that in (a) in the point that the spectral feature changes from LE-PL to SE with the excitation power. However, the intensity of SE increases with stress for each excitation power; in the spectra for 46.8 kW/cm^2 (SCD of 5.3×10^{11} cm^{-2}) shown by the thick lines, SE appears in (c) while not in (a). It is clear that the application of stress gives rise to a reduction of the SE threshold. In this power range, the peak energy of SE does not change with the excitation power and is below the mobility edge. Each downward arrow shows the energy position of the mobility edge, which was obtained from the dependence of the peak energy of PL spectrum on the excitation photon energy; the peak energy moves when the excitation energy is tuned below the mobility edge.[23,24] The relation between the mobility edge and the peak energy of SE will be discussed in the following section.

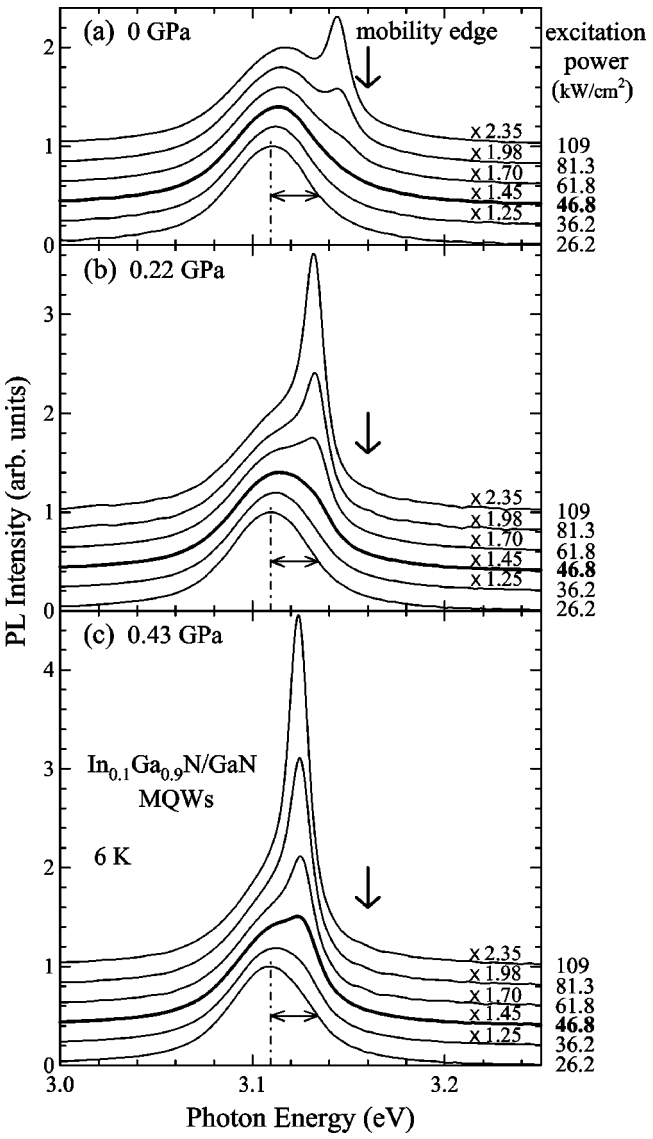

FIG. 3. PL spectra in $In_{0.1}Ga_{0.9}N$/GaN MQW's measured at 6 K under uniaxial stress of 0 GPa (a), 0.22 GPa (b), and 0.43 GPa (c). The spectra for the excitation powers from 26.2 kW/cm^2 to 109 kW/cm^2 are displayed. The peak intensities for 26.2 kW/cm^2 are set to unity. Each downward arrow indicates the energy position of the mobility edge.

Figure 4 shows the excitation power dependence of the peak intensity of spectra in Fig. 3. Logarithmic scales are used for both axes. Solid and open circles correspond to the results for a uniaxial stress of 0 GPa and 0.43 GPa, respectively. The dependence in each case is described with two lines as shown by thin and thick lines. In the region of low excitation power, the LE-PL is dominant and the peak intensities are proportional to $P^{0.63}$ for 0 GPa and $P^{0.72}$ for 0.43 GPa. Above 88 kW/cm^2 (1.0×10^{12} cm^{-2}) for 0 GPa and 48 kW/cm^2 (5.4×10^{11} cm^{-2}) for 0.43 GPa, due to the generation of SE, the peak intensities are proportional to $P^{1.9}$ and $P^{2.1}$, respectively. The excitation power at the intersection point of thin and thick lines, P_s, can be taken as the power at which the spectrum changes from LE-PL to SE.

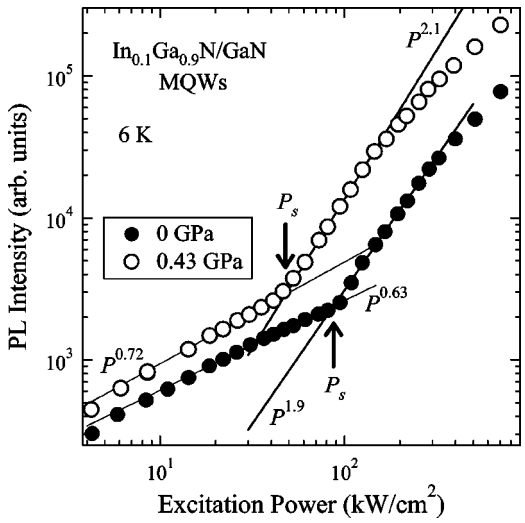

FIG. 4. Peak intensity of the PL spectrum in Fig. 3 plotted against the excitation power. Solid and open circles correspond to results under a uniaxial stress of 0 GPa and 0.43 GPa, respectively.

Figure 5 shows the P_s plotted against the uniaxial stress. P_s reduces as the uniaxial stress increases; the P_s at 0.43 GPa is 55% of that at 0 GPa.

In quantum well structures of wurtzite materials, a biaxial strain is known to occur in the active layer due to the difference of lattice constants between well and barrier layers, and the strain gives rise to a piezoelectric field.[25,27,28] This effect influences the PL characters such as the energy position and decay time, but the field is screened with increasing the density of photoexcited carriers. Takeuchi *et al.* showed that the lattice constant of underlying GaN layer is maintained in $In_{0.13}Ga_{0.87}N$ even with the well thickness up to 40 nm.[25] According to their result, the compression in the *c* plane of active layers in the present sample, $In_{0.1}Ga_{0.9}N/GaN$, is estimated to be 1.13%. The estimated biaxial stress and piezoelectric field are 5.26 GPa and 8.13×10^5 V/cm, respectively. Kuokstis *et al.* showed that the piezoelectric field of active

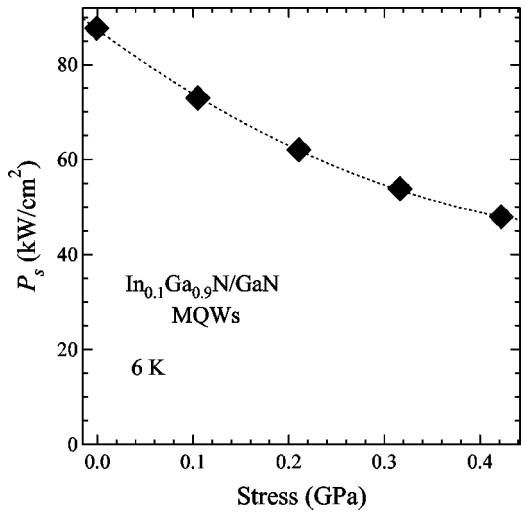

FIG. 5. Excitation power at the intersection of thin and thick lines in Fig. 4 (P_s) plotted against the stress.

layers in $In_{0.15}Ga_{0.85}N/GaN$ with well thickness of 4 nm is completely canceled by the screening effect due to carriers excited by the N_2 laser with 20 kW/cm^2.[28] Since the In content and well thickness in our sample are both lower than this case, the Stark effect should be weaker.[25,27] Application of uniaxial stress also induces a piezoelectric field along the *c* axis, which is estimated to be 7.28×10^4 V/cm^2 for 0.43 GPa as much as 9% of the background one. It may be clear from these estimates that each excitation power in Fig. 3 is enough to cancel the piezoelectric effect.

The stress effect observed here could be attributed to a change of valence-band structure similar to the case of GaN. The density of states at the valence-band maximum is reduced due to the increase in the energy splitting between *A* and *B* bands, and the SCD necessary to the population inversion becomes lower. As the result, the threshold SCD of SE decreases.

C. Optical gain without stress in InGaN/GaN MQW's

To examine the change of SE efficiency, a measurement of optical gain is required. The gain value *g* is available using the relation for amplified spontaneous emission measured with the variable-stripe method,

$$I=\frac{I_0}{g}\{\exp(gl)-1\}, \tag{3}$$

where *l* stands for the stripe length and I_0 and *I* for the intensities of spontaneous emission and amplified spontaneous emission, respectively.[31,33,34] At the long stripe length, however, *I* does not obey Eq. (3) due to the saturation effect, and the difference between Eq. (3) and experimental results increases with the stripe length. We use the following relation in which a saturation term in proportion to *I* is added to Eq. (3):

$$gl=\alpha I+\log\left(\frac{g}{I_0}I+1\right), \tag{4}$$

where α stands for the saturation parameter.[33]

PL spectra in $In_{0.1}Ga_{0.9}N/GaN$ MQW's were measured at 6 K with changing the stripe length from 6.7 μm to 1.2 mm. Optical gain is obtained from Eq. (4) by fitting the PL intensities against the stripe length. The gain values are plotted by solid circles in Fig. 6. Some PL spectra are shown by solid curves for reference. The vertical dotted lines stand for the mobility edge shown in Fig. 3. The excitation power in (a) is 91.4 kW/cm^2, and that in (b) is 1.84 MW/cm^2. As mentioned in the previous section, the Stark effect due to the background piezoelectric field must be negligible under these excitation powers. Equation (4) was able to apply up to 1.2 mm of the stripe length in (a), while was to 0.1 mm in the case of (b). Above these lengths, the saturation effect was too large to be approximated by Eq. (4). In (a), PL with a single band is observed for the shortest stripe length (0.10 mm). The structure corresponding to SE appears above 0.49 mm and increases with stripe length at the high-energy side of PL, and a positive optical gain is observed at the energy of SE. The peak energy of the gain is 3.152 eV, which is lower

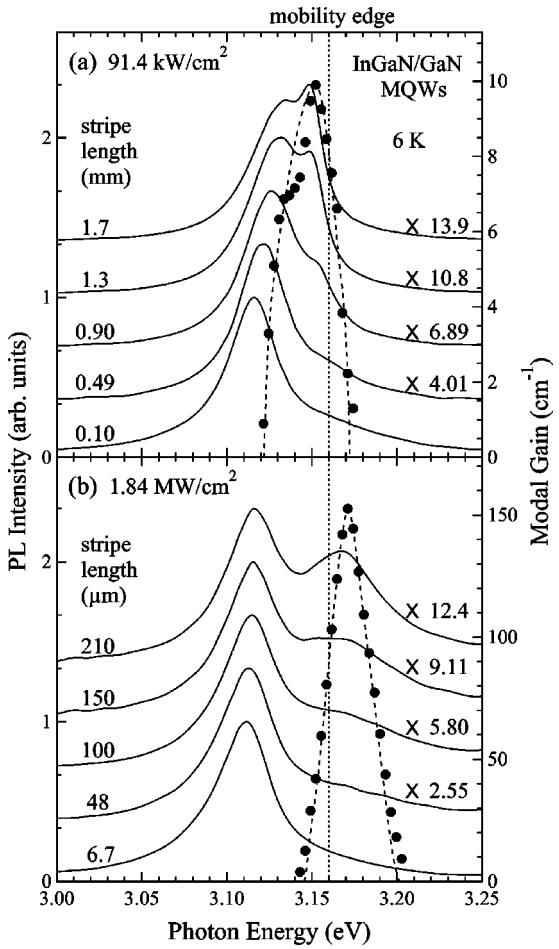

FIG. 6. PL and gain spectra measured with the variable-stripe method at 6 K in $In_{0.1}Ga_{0.9}N$/GaN MQW's. Solid lines show the PL spectra for various stripe lengths, and solid circles show the gain spectrum. Vertical dotted lines show the mobility edge. The excitation power is 91.4 kW/cm^2 in (a) and is 1.84 MW/cm^2 in (b).

than the mobility edge. The SCD is estimated to be 1.0×10^{12} cm^{-2}. Since the density is lower than the two-dimensional Mott-threshold density of excitons, 9.8×10^{12} cm^{-2}, an *e-h* plasma may not be generated as far as the uniform carrier distribution is assumed.[29] Satake *et al.* observed a SE in InGaN MQW's using time-resolved pump-probe measurements with excitation power below the threshold of *e-h* plasma and showed that *e-h* pairs excited in delocalized states relax into localized states, in which excitons are formed in a few picoseconds.[29] They concluded that optical gain is possible in terms of the SE process in the localized states due to the rapid relaxation. The result in Fig. 6(a) indicates that the SE process takes place in the localized states.

The peak of gain as well as of SE, which lies below the mobility edge in (a), shifts to higher energy with excitation power. The shift is ascribed to an increase in energy at which effective population inversion is achieved due to band filling of the localized states. The peak energy becomes constant when it reaches above the mobility edge. This suggests that the average SCD exceeds the total density of localized states and population inversion is achieved in delocalized states with large state density. In order to get SE in the delocalized states, the SCD should be larger than the two-dimensional Mott density of excitons; in the SCD higher than the threshold density of *e-h* plasma (9.8×10^{12} cm^{-2}) the recombination of *e-h* plasma takes place and contributes to SE. In fact, in Fig. 6(b) the peak energy of SE is higher than the mobility edge. The estimated SCD is 2.1×10^{13} cm^{-2}, which is higher than the threshold density of *e-h* plasma. Choi *et al.* studied carrier dynamics in InGaN thin film at 10 K using nondegenerate pump-probe spectroscopy and time-resolved PL and showed that SE occurs by the recombination of an *e-h* plasma from renormalized band-to-band transitions when the carrier density is higher than the total density of localized states.[35] The result in Fig. 6(b) indicates that *e-h* plasma recombination is the dominant process of SE when the SCD is above the threshold density.

However, the distinction between SE from PL of the localized states and that from *e-h* plasma recombination may not be clear. The localized state with energy close to the mobility edge is shallow and hence the size of the potential well is possibly large enough to contain more than one exciton. SE in these states could be the recombination of *e-h* plasma in the weak localized state as suggested by various authors.[26]

D. Optical gain with uniaxial stress in InGaN/GaN MQW's

Figure 7 shows PL and gain spectra measured under a uniaxial stress of 0.43 GPa. The gain values are plotted by solid circles, and several PL spectra are shown by thick solid curves. The gain without stress in Fig. 6 is displayed again by small open circles. The excitation powers are 91.4 kW/cm^2 in (a) and 1.84 MW/cm^2 in (b), the same as those in Fig. 6. In Fig. 7(a), for the case of low excitation power, the SCD is lower than the threshold density of *e-h* plasma and the gain peak is below the mobility edge. It is certain that SE is generated in the localized states, the same as in Fig. 6(a). It is found that the peak energy of gain as well as of SE shifts to 3.137 eV from that without stress (3.152 eV). This indicates that population inversion is attainable in the lower-energy states compared with the case without stress. The energy of SE in the tail states is governed by the relaxation time and density of states of localized excitons, both of which vary with energy. The stress-induced change in the density of states of each localized state may give rise to an apparent shift of the SE peak. The intensity of SE is enhanced by the applied stress as clearly seen in the spectra shown in Fig. 3. It seems that the low-energy shift of SE under stress improves the SE threshold. However, the change in the peak value of gain, 9.90 cm^{-1} in Fig. 6(a) and 11.0 cm^{-1} in Fig. 7(a), is marginal. These small values of gain are due to low excitation power which forces to a long stripe length and large saturation effect in deducing the gain value.

In Fig. 7(b), the peak energy of gain is 3.174 eV, almost the same as that in Fig. 6(b) (see open circles) and is higher than the mobility edge. It is certain that *e-h* plasma recombination is the dominant process of SE under the SCD of 2.1×10^{13} cm^{-2}. The maximum gain value is 205 cm^{-1},

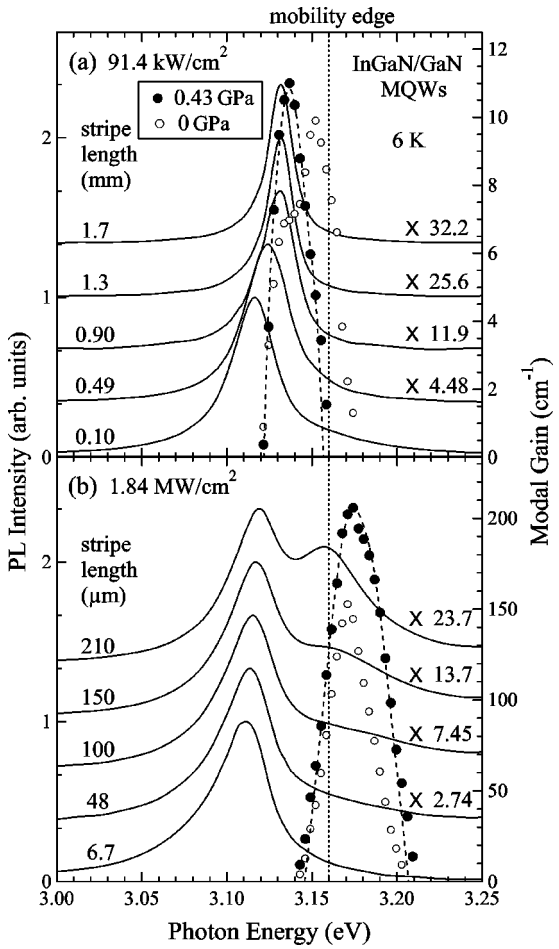

FIG. 7. PL and gain spectra measured under the uniaxial stress of 0.43 GPa at 6 K in $In_{0.1}Ga_{0.9}N/GaN$ MQW's. Solid lines, solid circles, and vertical dotted lines show the PL spectra for various stripe lengths, gain spectrum, and mobility edge, respectively. The excitation power is 91.4 kW/cm^2 in (a) and is 1.84 MW/cm^2 in (b). The gain spectra shown in Fig. 6 are displayed by small open circles for comparison.

which is 1.34 times as large as that in Fig. 6(b) (153 cm^{-1}). Suzuki and Uenoyama calculated the strain effect on the optical gain of wurtzite $GaN/Al_{0.2}Ga_{0.8}N$ quantum wells.[18–20] According to their calculation, the maximum gain is found to be 1.7 times as large as that without strain for SCD of 2.1 $\times 10^{13}$ cm^{-2} under the condition of 1% compressive uniaxial strain introduced to the sample with the same geometry as the present experiment. The estimated value of the compression in the present experiment with a uniaxial stress of 0.43 GPa is 0.30%. The increase in gain with the uniaxial stress in Fig. 7(b) is comparable with the theoretical estimation.

It is to be noted that there is a background strain, on which *c* surface is compressed of 1.13% biaxially as mentioned above. From the calculation in wurtzite $GaN/Al_{0.2}Ga_{0.8}N$ quantum wells by Suzuki and Uenoyama, the maximum gain under a biaxial strain of 0.5% is found to be 1.1 times as large as that without strain for SCD of 2.1 $\times 10^{13}$ cm^{-2}.[18–20] According to them, the gain may be increased in the order of 10% by the effect of background strain even without uniaxial strain.

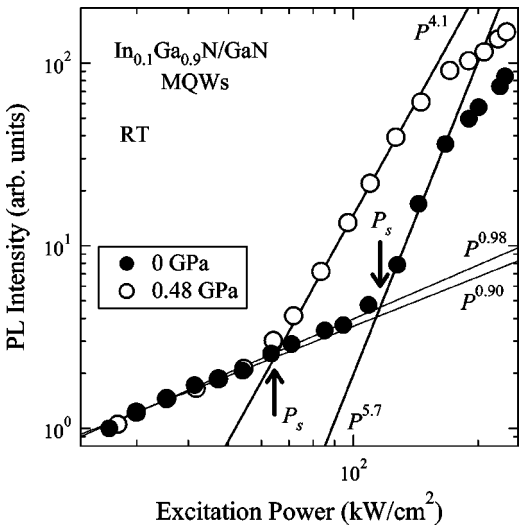

FIG. 8. Peak intensity of PL spectrum at room temperature in $In_{0.1}Ga_{0.9}N/GaN$ MQW's plotted against excitation power. Solid and open circles correspond to the results under a uniaxial stress of 0 GPa and 0.48 GPa, respectively.

It is concluded that uniaxial stress leads to an increase in the optical gain; the decrease in the threshold carrier density of SE in InGaN/GaN MQW's in both the LE state and the *e-h* plasma. This is ascribed to a decrease in the density of states at the valence-band top induced by the uniaxial stress.

E. Result at room temperature

The PL spectrum of $In_{0.1}Ga_{0.9}N/GaN$ MQW's at room temperature (RT) has a peak at 3.11 eV, a little lower than that at 6 K, and the bandwidth is about 2.5 times broader. The SE peak grows at 3.12 eV with increasing excitation power. Figure 8 shows the excitation power dependence of the peak intensity of PL spectrum at RT. The experimental configurations are the same as those in Fig. 4. The value of

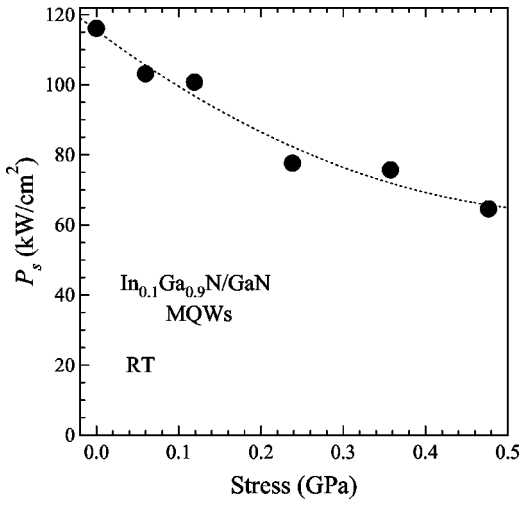

FIG. 9. Excitation power at the intersection of thin and thick lines in Fig. 8 (P_s) plotted against stress.

P_s for 0 GPa is about 1.3 times higher than that at 6 K. The increase in the SE threshold is not so large in spite that the PL efficiency decreases to about an order of magnitude, similar to the results already reported.[24] The excitation power in which the spectrum changes from LE-PL to SE is clearly reduced by the introduction of uniaxial stress similar to Fig. 4. Figure 9 shows the stress dependence of P_s. The critical power value decreases monotonically as the stress increases similar to Fig. 5. The P_s for 0.48 GPa in Fig. 9 decreases to 55% of that for 0 GPa. The efficiency of reduction in the threshold carrier density of SE at RT is almost the same as that at 6 K. Satake *et al.* reported from a pump-probe experiment that the SE mechanism at RT is the same as that at 2 K; namely, the PL from the localized excitons (localized carriers) contributes to SE.[29] The peak energy of SE did not show the high-energy shift with the increase in the SCD as observed at 6 K. The distinction between localized and delocalized states may not be clear due to the thermalization effect. Though the gain values were difficult to obtain due to the high saturation effect at RT, the present result tells us that the advantage brought by the application of uniaxial stress is expected not only at low temperatures but at RT where device applications are attempted.

IV. SUMMARY

The dependence of the PL spectrum on uniaxial stress in a GaN bulk crystal shows that the energy splitting between *A* and *B* excitons increases and the PL intensity of *B* excitons relative to that of *A* excitons decreases with increasing stress. The carrier density necessary for SE to appear in InGaN/GaN MQW's is reduced by the uniaxial stress at both 6 K and RT. From the measurement of optical gain, it is found that SE is generated in localized states in low excitation power and from *e-h* plasma recombination in higher excitation power above the Mott density. In the latter case, the maximum gain value at 0.43 GPa stress is 1.34 times as large as that without stress and the increasing rate is consistent with a theoretical estimation. A favorable effect of stress is observed also at RT.

[1] M. Ogura and T. Yao, J. Vac. Sci. Technol. B **3**, 784 (1985).
[2] H. Kawanishi and N. Tsuchiya, J. Appl. Phys. **58**, 37 (1985).
[3] M. Ishikawa, Y. Ohba, H. Sugawara, M. Yamamoto, and T. Nakanishi, Appl. Phys. Lett. **48**, 207 (1986).
[4] S. Nakamura, J. Vac. Sci. Technol. A **13**, 705 (1995).
[5] S. Nakamura, M. Senoh, N. Iwasa, and S. Nagahama, Appl. Phys. Lett. **67**, 1868 (1995).
[6] S. Nakamura, M. Senoh, S. Nagahama, N. Iwasa, T. Yamada, T. Matsushita, H. Kiyoku, and Y. Sugimoto, Jpn. J. Appl. Phys., Part 2 **35**, L74 (1996).
[7] S. Nakamura, M. Senoh, S. Nagahama, N. Iwasa, T. Yamada, T. Matsushita, H. Kiyoku, and Y. Sugimoto, Appl. Phys. Lett. **68**, 2105 (1996).
[8] M. Suzuki and T. Uenoyama, Appl. Phys. Lett. **69**, 3378 (1996).
[9] S. Chichibu, T. Azuhata, T. Sota, and S. Nakamura, Appl. Phys. Lett. **70**, 2822 (1997).
[10] W. Fang and S.L. Chuang, Appl. Phys. Lett. **67**, 751 (1995).
[11] A.T. Meney and E.P. O'Reilly, Appl. Phys. Lett. **67**, 3013 (1995).
[12] S. Kamiyama, K. Ohnaka, M. Suzuki, and T. Uenoyama, Jpn. J. Appl. Phys., Part 2 **34**, L821 (1995).
[13] M. Suzuki and T. Uenoyama, Phys. Rev. B **52**, 8132 (1995).
[14] M. Suzuki and T. Uenoyama, Jpn. J. Appl. Phys., Part 1 **35**, 543 (1996).
[15] M. Suzuki and T. Uenoyama, Solid-State Electronics **41**, 271 (1997).
[16] T. Uenoyama and M. Suzuki, Appl. Phys. Lett. **67**, 2527 (1995).
[17] M. Suzuki and T. Uenoyama, Jpn. J. Appl. Phys., Part 1 **35**, 1420 (1996).
[18] M. Suzuki and T. Uenoyama, J. Appl. Phys. **80**, 6868 (1996).
[19] M. Suzuki and T. Uenoyama, Jpn. J. Appl. Phys., Part 2 **35**, L953 (1996).
[20] M. Suzuki and T. Uenoyama, in *Gallium Nitride and Related Materials II*, edited by C. R. Abernathy, H. Amano, and J. C. Zolper , Mater. Res. Soc. Symp. Proc. No. **468** (Materials Research Society, Pittsburgh, 1997), p. 251.
[21] A.A. Yamaguchi, Y. Mochizuki, C. Sasaoka, A. Kimura, M. Nido, and A. Usui, Appl. Phys. Lett. **71**, 374 (1997).
[22] K. Domen, K. Horino, A. Kuramata, and T. Tanahashi, Appl. Phys. Lett. **70**, 987 (1997).
[23] A. Satake, Y. Masumoto, T. Miyajima, T. Asatsuma, F. Nakamura, and M. Ikeda, Phys. Rev. B **57**, R2041 (1998).
[24] Y.H. Cho, T.J. Schmidt, S. Bidnyk, G.H. Gainer, J.J. Song, S. Keller, U.K. Mishra, and S.P. DenBaars, Phys. Rev. B **61**, 7571 (2000).
[25] T. Takeuchi, S. Sota, M. Katsuragawa, M. Komori, H. Takeuchi, H. Amano, and I. Akasaki, Jpn. J. Appl. Phys., Part 2 **36**, L382 (1997).
[26] S.F. Chichibu, T. Sota, K. Wada, S.P. DenBaars, and S. Nakamura, MRS Internet J. Nitride Semicond. Res. **4S1**, G2.7 (1999), and references therein.
[27] A. Hangleiter, J. Lumin. **87-89**, 130 (2000).
[28] E. Kuokstis, J.W. Yang, G. Simin, M. Asif Khan, R. Gaska, and M.S. Shur, Appl. Phys. Lett. **80**, 977 (2002).
[29] A. Satake, Y. Masumoto, T. Miyajima, T. Asatsuma, and M. Ikeda, Phys. Rev. B **60**, 16 660 (1999).
[30] G. Frankowsky, F. Steuber, V. Härle, F. Scholz, and A. Hangleiter, Appl. Phys. Lett. **68**, 3746 (1996).
[31] G. Mohs, T. Aoki, N. Nagai, R. Shimano, M. Kuwata-Ganoakami, and S. Nakamura, Solid State Commun. **104**, 643 (1997).
[32] J.F. Muth, J.H. Lee, I.K. Shmagin, R.M. Kolbas, H.C. Casey, Jr., B.P. Keller, U.K. Mishra, and S.P. DenBaars, Appl. Phys. Lett. **71**, 2572 (1997).
[33] K.L. Shaklee, R.E. Nahory, and R.F. Leheny, J. Lumin. **7**, 284 (1973).
[34] A. Ishibashi, I. Kidoguchi, A. Tsujimura, Y. Hasegawa, Y. Ban, T. Ohata, M. Watanabe, and T. Hayashi, J. Lumin. **87-89**, 1271 (2000).
[35] C.K. Choi, B.D. Little, Y.H. Kwon, J.B. Lam, and J.J. Song, Phys. Rev. B **63**, 195302 (2001).